Development of Layered Multiscale Porous Thin Films by Tuning Deposition Time and Molecular Weight of Polyelectrolytes

Jing Yu, Oishi Sanyal, Andrew P. Izbicki, Ilsoon Lee*

This work focuses on the design of porous polymeric films with nano- and micro-sized pores existing in distinct zones. The porous thin films are fabricated by the post-treatment of layer-by-layer assembled poly(allylamine hydrochloride) (PAH)/poly(acrylic acid) (PAA) multilayers. In order to improve the processing efficiency, the deposition time is shortened to ≈10 s. It is found that fine porous structures can be created even by significantly reducing the processing time. The effect of using polyelectrolytes with widely different molecular weights is also studied. The pore size is increased by using high molecular weight PAH, while high molecular weight PAA minimizes the pore size to nanometer scale. Having gained a precise control over the pore size, layered multiscale porous thin films are further built up with either a microsized porous zone on top of a nanosized porous zone or vice versa.

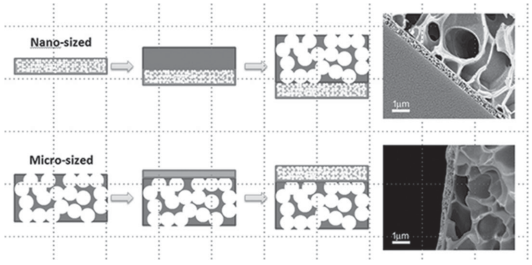

1. Introduction

Porous polymeric films are in demand for a wide range of applications including foams,[1] insulators,[2] membranes,[3] catalytic supports,[4] antireflection coatings,[5] superhydrophobic coatings,[6] and drug delivery systems.[7] For many applications, sophisticated porous structures with a precise control on the pore sizes ranging from nano- to micrometer are desired. For example, hierarchical (i.e., micro- and nano-sized) porous surfaces also help achieve superhydrophobicity.[8] For controlled drug release, the release rate is highly dependent on the pore size.[9] A well-controlled porous structure enables a tunable drug release over time.[10] In addition, commercial nanofiltration/reverse osmosis membranes have an asymmetric structure with two distinct types of porous zones; the bottom one consists of microsized pores while the upper zone consists of nanosized pores. Motivated by these prospects, the multiscale porous thin films with well-defined micro- and nanosized porous regions were developed in this work.

Layer-by-layer (LbL) assembly is considered as a highly versatile deposition technique for fabricating functional thin films and coatings.[11] LbL assembled polyelectrolyte multilayers (PEMs) followed by simple post-treatment steps provides one of the most promising methods to generate porous polymeric frameworks. Rubner and co-workers first demonstrated the formation of porous networks using poly(allylamine hydrochloride) (PAH)/poly(acrylic acid) (PAA) multilayers. The PEMs were fabricated with the PAH solution at a pH of 7.5 or 8.5 and the PAA solution at a pH of 3.5. The porous structure was formed after the post-treatment, which includes acidic immersion within the pH range of 1.8–2.6, rinsing in deionized (DI) water, drying and cross-linking.[5,6,9,12] Both nano- and micro-sized porous films were able to be achieved by tuning the post-treatment conditions. In addition, free-standing porous PAH/PAA films can be obtained through an ion-triggered exfoliation method.[12d] Porous thin films can also be fabricated by salt-induced

J. Yu, O. Sanyal, A. P. Izbicki, I. Lee
Department of Chemical Engineering and Materials Science
Michigan State University
East Lansing, MI 48824, USA
E-mail: leeil@egr.msu.edu

DOI: 10.1002/marc.201500250

structural changes in PAH/PAA multilayers.[13] The porous structures were formed by exposing the PAA/PAH multilayers fabricated in the presence of salt to pure water. However, the pore size was limited to the nanometer scale. Another way to make porous thin films via LbL assembly is through the treatment of hydrogen-bonded poly(4-vinylpyridine) (PVP)/PAA multilayers in aqueous solution at pH of 12.5 when PAA was dissolved followed by the reconfirmation of PVP chains.[14] Only microsized pores were obtained, and the stability of the hydrogen-bonded LbL films over a broad range of pH is always an issue. Thus, in this work, we applied acidic treatment to induce the porous formation in PAH/PAA multilayer films.

Immersion of PAH/PAA films in a low-pH aqueous solution causes rearrangement of the polymer chains.[5,12b,c] This rearrangement is induced by the breakage of the ionic cross-links of PAA due to protonation of the carboxylate groups and charge repulsion among the free, positively charged amine groups of PAH. The rinsing step with DI water allows ion pairs to reform and form small water pockets by rejecting water from the film. By drying water out from the water pockets and cross-linking the polymer chains, stable porous films were obtained.

In order to create distinct zones with different scales of the pore size, the prerequisite was to have a very precise control on each of the zones independently and to understand the factors that affect the formation of those zones. Once those factors were identified, their combination could lead us to form multiscale porous frameworks. Previous studies mainly investigated the effect of the number of layers[12a,d], pH[5], [9,12a,c,15] and time [12a,d,15a] of the post-treatment on the morphology of the porous PAH/PAA films. However, one major obstacle in commercializing any of these films is the long processing time that goes into fabricating the PAH/PAA films using LbL technique. Recently, several studies initiated using short deposition time to address this issue and apply for gas barrier films.[16] The deposition time was shortened from conventional 15–20 min to less than 1 min. It has been found that different deposition time leads to varied film compositions and structures.[16a] Since the formation of porous PAH/PAA films is mainly dependent on the interaction between PAA and PAH and the reorganization of polymer chains, the changes in film composition and polymer distribution may further alter the porous structure. However, no research has been focused on studying the effect of deposition time on the porous structure or how efficiently the porous thin films can be built up. In addition, the mobility of the individual polymer chains also plays a crucial role. During the post-treatment, the reorganization of polymer chains is highly influenced by the chain mobility and the interaction among functional groups. In this regard, the molecular weight of polyelectrolytes could be one of the critical and intrinsic parameters to tune the porous structure since it highly affects the chain mobility and the intramolecular and intermolecular interactions. It has been reported that the molecular weight of polyelectrolytes plays an important role during LbL assembly.[17] However, few studies focused on the molecular weight effect of polyelectrolytes on the porous structure.[15b] In order to study the molecular weight effect thoroughly, we fabricated PAH/PAA multilayers using PAA with molecular weight of 15 000 g mol^{-1} (PAA_L) and 225 000 g mol^{-1} (PAA_H) and PAH with molecular weight of 15 000 g mol^{-1} (PAH_L) and 900 000 g mol^{-1} (PAH_H). In this study, we focused on the effect of deposition time and molecular weight of polyelectrolytes on the porous morphology in order to shorten the fabrication time and obtain a wider and more precise control on the porous structure at the same time.

2. Results and Discussion

In this work, the PAH/PAA multilayers were constructed by the alternate deposition of PAH at pH = 8.5 and PAA at pH = 3.5. According to the literature, the degree of ionization of PAA in aqueous solution with pH = 3.5 is less than 10%,[18] while the degree of ionization of PAH in aqueous solution with pH = 8.5 is around 50%.[18a,19] Under this pH condition, a high level of interlayer diffusion occurs in order for charge compensation to take place, leading to an exponential growth in the thickness of the multilayer films.[18b,20] The variations in the thickness of $(PAH_L/PAA_L)_{20.5}$ films as a function of the deposition time are shown in Figure 1a. The deposition time varies from 10 s to 15 min. Before the post-treatment, the multilayer thickness increases with the increase in deposition time as a result of time-dependent interdiffusion process. For short deposition time, the interlayer diffusion is suppressed, leading to thinner multilayers. This result is consistent with several previous studies.[16a,20] When the deposition time was increased from 10 to 15 min, the thickness almost remained the same. In fact, besides the change in thickness, the composition and distribution of PAA and PAH in the multilayers were also altered by deposition time.[16a] All these factors affect the breakage of the ionic cross-links and the rearrangement of polymer chains, leading to different porous structures. The acid treatment was carried out under the condition of pH = 2.0 for 5 min followed by 5 min of washing step with DI water. The porous structure was then thermally cross-linked at 180 °C for 2 h. The entire post-treatment protocol was maintained the same throughout this study. Figure S1 (Supporting Information) shows the SEM images of the surface and cross section of the porous structure with different deposition time. The values of average surface pore size are summarized in Figure 1b. The average surface pore size increased sharply from 108 to 259 nm when the deposition time changed from 10 s to 1 min. With deposition time

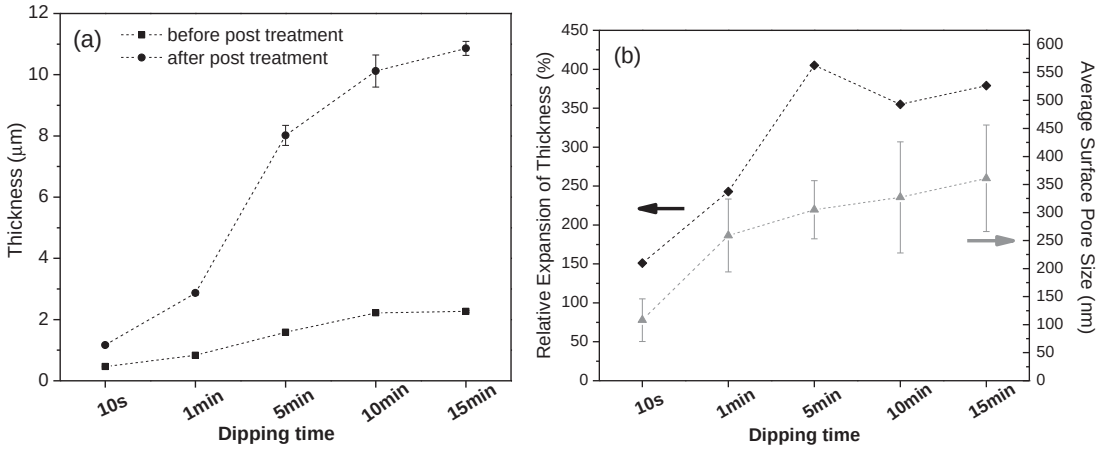

Figure 1. The effect of deposition time on a) the thickness of PAH_L/PAA_L thin films before and after the post-treatment and b) the relative expansion of thickness and average surface pore size.

further increased to 5, 10, and 15 min, the average surface pore size increased to 305, 327, and 361 nm, respectively. In general, longer deposition time created larger surface pore size. It is also obvious from Figure S1 (Supporting Information) that the inner pore size is different than the surface pore size. Microsized pores were successfully formed throughout the entire cross section of the films. It is hard to measure the actual inner pore size, because the pores were highly interconnected. However, it is still obvious that the inner pore size increased as the dipping prolonged from 10 s to 1 min. Figure 1b also shows the relative expansion of thickness as a function of deposition time. The value is not always proportional to the deposition time. This indicates that several intertwined factors like film composition, polyelectrolyte distribution, the nature of polyelectrolytes (i.e., chain mobility and hydrophilicity), mass lost during the post-treatment[15a], etc., influence the porous structure in a synergistic manner. The interlayer diffusion during LbL assembly definitely facilitated the formation of pores. Even though there are certain differences in thickness and pore size, the porous structures are very similar to each other when deposition time is longer than 5 min. Proper porous structure could be generated by the PAH_L/PAA_L multilayers assembled with deposition time of 10 s in a much faster way and with a smaller pore size.

Considering the efficiency of fabricating porous films, 10 s dipping was further applied to different molecular weight systems in order to study the molecular weight effect on the porous morphology. The acid treatment was still carried out by immersing PAH/PAA multilayers in pH = 2.0 aqueous solution for 5 min followed by 5 min of washing with DI water. Figure 2a illustrates the effect of molecular weight on the thickness of the films before and after post-treatment. Before porous treatment, the thickness for $(PAH_L/PAA_L)_{20.5}$ is almost the same as $(PAH_H/PAA_L)_{20.5}$. Similar results were also found for $(PAH_L/PAA_H)_{20.5}$ and $(PAH_H/PAA_H)_{20.5}$ films, which means the molecular weight of PAH does not affect the thickness of the films significantly. However, high molecular weight of PAA led to a decrease in thickness for multilayers

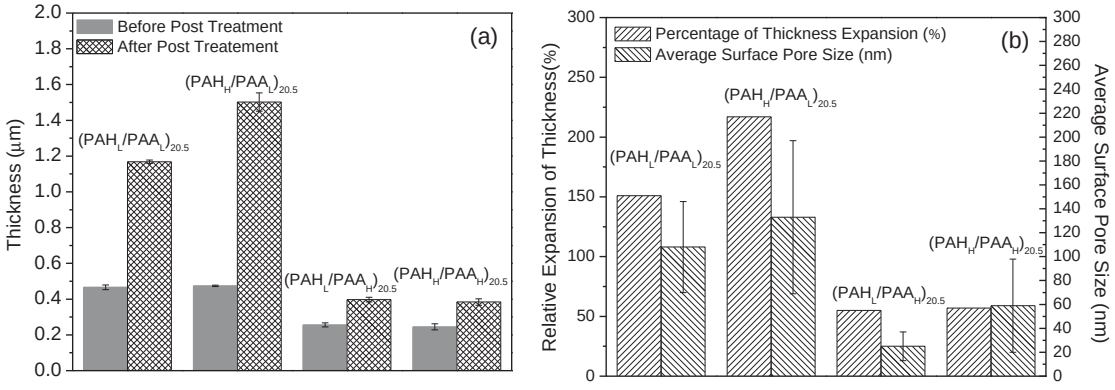

Figure 2. a) Thickness of thin films before and after the post-treatment and b) the relative expansion of thickness and average surface pore size for $(PAH_L/PAA_L)_{20.5}$, $(PAH_H/PAA_L)_{20.5}$, $(PAH_L/PAA_H)_{20.5}$, and $(PAH_H/PAA_H)_{20.5}$, respectively. All the films were fabricated using deposition time of 10 s.

fabricated using the same molecular weight of PAH. After the post-treatment, the relative expansion of thickness for $(PAH_L/PAA_L)_{20.5}$, $(PAH_H/PAA_L)_{20.5}$, $(PAH_L/PAA_H)_{20.5}$, and $(PAH_H/PAA_H)_{20.5}$ are shown in Figure 2b, respectively. With the same molecular weight of PAA, high molecular weight of PAH provided higher relative expansion of thickness; while with same molecular weight of PAH, high molecular weight of PAA limited the thickness expansion during the post-treatment. SEM images for all four porous thin films are shown in Figure S2 (Supporting Information). It is obvious from the top view images in Figure S2 (Supporting Information) that high molecular weight of PAH not only creates larger surface pore size but also leads to a less uniform pore size distribution. In addition, high molecular weight PAA lowers the pore size significantly, which is consistent with what has been reported previously.[15b] The values of average surface pore size are presented in Figure 2b. The surface pore size could be tuned from 25 to 133 nm with different molecular weight combinations. Similar results can also be obtained for the inner pore size from the cross-sectional images in Figure S2 (Supporting Information), that high molecular weight of PAA led to a decrease in the inner pore size, while high molecular weight of PAH provided larger inner pores. According to the previous studies,[12b,c] when PAH/PAA multilayers are immersed in pH = 2.0 aqueous solution, the carboxylate groups from PAA are protonated leading to the breakage of ionic cross-links, while the amine groups from PAH become fully charged. The intramolecular charge–charge repulsion for high molecular weight of PAH is much stronger than that of low molecular weight of PAH. This explains why the high molecular weight PAH caused larger pore size as well as higher relative expansion of thickness. Besides, the reorganization of polymer chain during post-treatment is highly dependent on the chain mobility of the polyelectrolytes. PAA has very low charge density when immersed in pH = 2.0 aqueous solution. The chain mobility is highly limited by using higher molecular weight of PAA, leading to a smaller pore size and consequently a lower relative expansion of thickness. It is apparent that the molecular weight of the polyelectrolytes plays a very important role in the formation of porous structures. However, the molecular weight effect does not only exist during the post-treatment. During the LbL assembly, the molecular weight of polyelectrolytes also affects the adsorption and interlayer diffusion, leading to different film composition and distribution of polyelectrolytes.[17b,d,21] It is hard to differentiate how these factors affect the porous structure independently, even though the deposition time of 10 s was applied when the interlayer diffusion is highly limited. But from the above results, there is no doubt that changing molecular weight of polyelectrolytes enables a wider control of pore size and morphology.

Based on the porous structures described above, multiscale porous films were fabricated which constituted of a macrosized porous zone on top of nanosized porous zone (Figure 3) or the other way around (Figure 4). To fabricate these films, the bottom porous portion was made first using the usual protocol of LbL assembly followed by the post-treatment. The PAA and PAH chains were completely reorganized during the acid immersion and DI water rinsing step, leaving both COO^- groups and NH_3^+ groups on the surface. The cross-linking step causes the formation of amide bonds (—NHCO—) between the COO^- groups of PAA and NH_3^+ of PAH and preserves the porous structure from being altered by further immersion in aqueous solution.[12c,22] Some free carboxylate groups and ammonium groups remained in the films after the cross-linking.[22] The remaining free ammonium groups on the surface enabled the deposition of PAA at pH 3.5, when ammonium groups are completely charged and carboxylate groups become mostly protonated. The bottom porous thin film thereby acted as the substrate to further build up porous films on the top. Considering the quality of the porous structure and the fabrication efficiency,

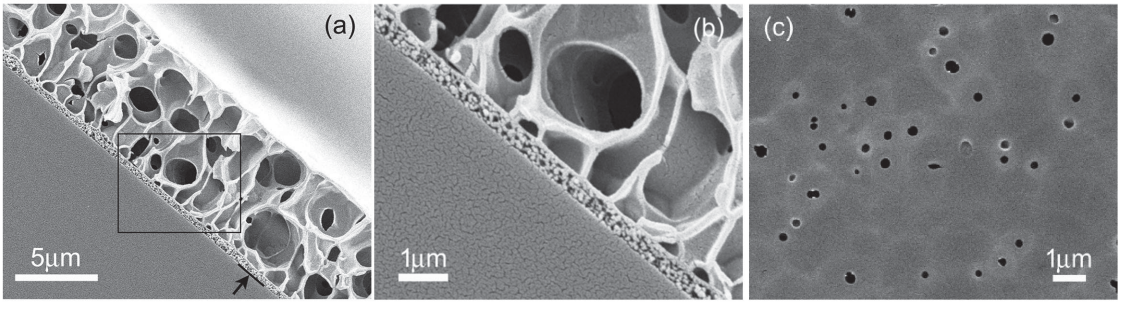

Figure 3. SEM a,b) cross-sectional and c) top view images of multiscale porous thin film with nanosized porous film as the bottom and microsized porous film as the top. The arrow in (a) indicates the interface between the glass substrate and the deposited film. (b) is an enlarged image of the square area in (a). The multiscale porous thin films were made through the following protocol. The porous $(PAH_L/PAA_H)_{20.5}$ thin film with deposition time of 10 s was first built up as the bottom portion. $(PAA_L/PAH_L)_{20}$ thin film with deposition time of 5 min was further built up and made porous as the top portion of this multiscale porous structure.

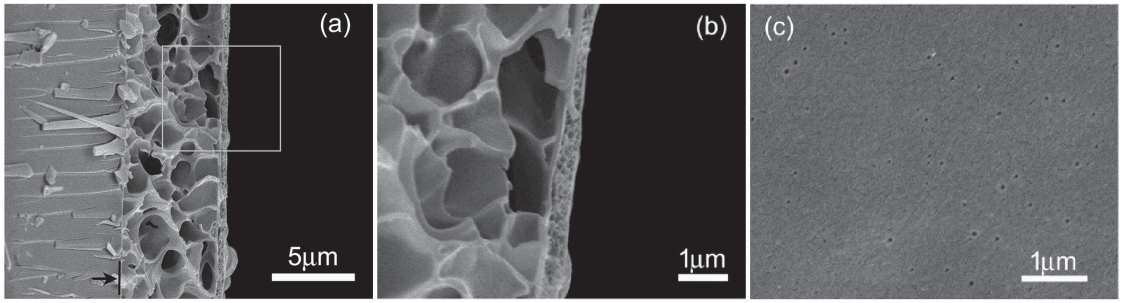

Figure 4. SEM a,b) cross-sectional and c) top view images of multiscale porous thin film with microsized porous structure as the bottom and nanosized porous structure as the top. The arrow in (a) indicates the interface between the glass substrate and the deposited film. (b) is an enlarged image of the square area in (a). The multiscale porous thin films were made through the following protocol. The porous $(PAA_L/PAH_L)_{20.5}$ thin film with deposition time of 5 min was first built up as the bottom portion. $(PAH_L/PAA_H)_{20}$ thin film with deposition time of 10 s was further built up and made porous as the top portion of this multiscale porous structure.

porous PAH_L/PAA_L thin film with 5 min dipping was selected as the microsized porous portion, while porous PAH_L/PAA_H thin film with deposition time of 10 s was chosen as the nanosized porous portion.

As shown in Figure 3, porous $(PAH_L/PAA_H)_{20.5}$ thin film with deposition time of 10 s was first built up as the bottom portion, followed by the porous $(PAA_L/PAH_L)_{20}$ thin film with deposition time of 5 min. Two clearly defined zones with different pore sizes were fabricated by this method, without any significant penetration of polyelectrolytes into the nanosized bottom portion. In addition, the surface and cross-sectional morphology for microsized top zone of the multiscale porous films remained almost the same as the simple porous $(PAH_L/PAA_L)_{20.5}$ films with deposition time of 5 min (Figure S1e,f, Supporting Information). Hence, the substrate effect was minimal for the microsized porous top zone.

In the above mentioned scenario, the underlying porous portion had very small surface pore size, therefore the molecular weight of the polyelectrolytes used to build up the top porous portion, is not a matter of serious concern. However, if the bottom portion is made with relatively larger surface pore size, PAA with high molecular weight is required for the top porous portion. This is because the polymer chain size needs to be large enough to prevent diffusion into the porous bottom. In addition, after the bottom portion was thermally cross-linked, the surface became more hydrophobic, which helped trap air inside the porous structure and block the polyelectrolytes outside. As shown in Figure 4a,b, nanosized porous structure of $(PAA_H/PAH_L)_{20}$ with 10 s dipping has been successfully fabricated on top of the porous $(PAH_L/PAA_L)_{20.5}$ films with deposition time of 5 min. It is clear that no polyelectrolytes entered into the microsized porous bottom. Figure 4c shows the top view of this particular multiscale porous thin film. Compared to Figure S2e (Supporting Information), it has been found that the number of pores decreases, while the pore size increases to 50 ± 19 nm. There was a slight change in the porous morphology for the nanosized porous region of the multiscale porous thin film from the simple porous $(PAA_H/PAH_L)_{20}$ film with 10 s dipping. This is mainly because the microsized porous bottom has different charge density than the plasma treated glass slides, and the substrate effect is relatively more obvious when the film is very thin.

3. Conclusion

In summary, multiscale porous thin films have been developed for the first time with either microsized porous structure on top of nanosized porous structure or vice versa. In order to build up the porous thin films more efficiently, the effect of deposition time on the morphology of porous films was investigated for the first time in this work. Compared to conventional 15 or 20 min dipping, we were able to shorten the deposition time to 10 s but still maintain fine porous structures. The molecular weight effect of both PAH and PAA was also studied. While an increase in the molecular weight of PAH led to an increase in the pore size, a decrease in the pore size was observed for a high molecular weight of PAA. The layered multiscale porous thin films were further fabricated by tuning the deposition time and molecular weight of polyelectrolytes. The porous thin films developed in the present work may broaden the applications of porous thin films for membrane filtration, drug delivery, etc.

Supporting Information

Supporting Information is available from the Wiley Online Library or from the author.

Acknowledgements: The funding from the MSU Foundation (Strategic Partnership Grant) and the DOD Strategic Environmental Research and Development Program (DOD SERDP W912HQ-12-C-0020) is greatly appreciated.

The axis labels for Figure 1 were corrected on September 15, 2015.

Received: April 28, 2015; Revised: June 1, 2015; Published online: July 14, 2015; DOI: 10.1002/marc.201500250

Keywords: multi-scale porous films; layer by layer; polyelectrolytes; polymers; deposition time; molecular weight

[1] S. K. Goel, E. J. Beckman, *Polym. Eng. Sci.* **1994**, *34*, 1137.
[2] C. V. Nguyen, K. R. Carter, C. J. Hawker, J. L. Hedrick, R. L. Jaffe, R. D. Miller, J. F. Remenar, H.-W. Rhee, P. M. Rice, M. F. Toney, *Chem. Mater.* **1999**, *11*, 3080.
[3] a) O. Sanyal, A. N. Sommerfeld, I. Lee, *Sep. Purif. Technol.* **2015**, *145*, 113; b) O. Sanyal, I. Lee, *J. Nanosci. Nanotechnol.* **2014**, *14*, 2178.
[4] F. Svec, J. M. Fréchet, *Science* **1996**, *273*, 205.
[5] J. A. Hiller, J. D. Mendelsohn, M. F. Rubner, *Nat. Mater.* **2002**, *1*, 59.
[6] L. Zhai, F. C. Cebeci, R. E. Cohen, M. F. Rubner, *Nano Lett.* **2004**, *4*, 1349.
[7] D. A. Edwards, J. Hanes, G. Caponetti, J. Hrkach, A. Ben-Jebria, M. L. Eskew, J. Mintzes, D. Deaver, N. Lotan, R. Langer, *Science* **1997**, *276*, 1868.
[8] J. Fu, J. Ji, L. Shen, A. Küller, A. Rosenhahn, J. Shen, M. Grunze, *Langmuir* **2008**, *25*, 672.
[9] M. C. Berg, L. Zhai, R. E. Cohen, M. F. Rubner, *Biomacromolecules* **2006**, *7*, 357.
[10] S. B. Yoon, K. Sohn, J. Y. Kim, C.-H. Shin, J.-S. Yu, T. Hyeon, *Adv. Mater.* **2002**, *14*, 19.
[11] a) G. Decher, *Science* **1997**, *277*, 1232; b) R. Iler, *J. Colloid Interface Sci.* **1966**, *21*, 569; c) I. Lee, *Langmuir* **2013**, *29*, 2476.
[12] a) C. Sung, Y. Ye, J. L. Lutkenhaus, *ACS Macro Lett.* **2015**, *4*, 353; b) K.-K. Chia, M. F. Rubner, R. E. Cohen, *Langmuir* **2009**, *25*, 14044; c) J. Mendelsohn, C. J. Barrett, V. Chan, A. Pal, A. Mayes, M. Rubner, *Langmuir* **2000**, *16*, 5017; d) X. Chen, J. Sun, *Chem. - Asian J.* **2014**, *9*, 2063.
[13] A. Fery, B. Schöler, T. Cassagneau, F. Caruso, *Langmuir* **2001**, *17*, 3779.
[14] a) S. Bai, Z. Wang, X. Zhang, B. Wang, *Langmuir* **2004**, *20*, 11828; b) Y. Fu, S. Bai, S. Cui, D. Qiu, Z. Wang, X. Zhang, *Macromolecules* **2002**, *35*, 9451.
[15] a) C. Cho, N. S. Zacharia, *Langmuir* **2011**, *28*, 841; b) B. Sun, R. M. Flessner, E. M. Saurer, C. M. Jewell, N. J. Fredin, D. M. Lynn, *J. Colloid Interface Sci.* **2011**, *355*, 431.
[16] a) D. A. Hagen, B. Foster, B. Stevens, J. C. Grunlan, *ACS Macro Lett.* **2014**, *3*, 663; b) Y.-H. Yang, F. A. Malek, J. C. Grunlan, *Ind. Eng. Chem. Res.* **2010**, *49*, 8501.
[17] a) S. T. Dubas, J. B. Schlenoff, *Macromolecules* **2001**, *34*, 3736; b) C. Porcel, P. Lavalle, G. Decher, B. Senger, J.-C. Voegel, P. Schaaf, *Langmuir* **2007**, *23*, 1898; c) Y. Jang, J. Seo, B. Akgun, S. Satija, K. Char, *Macromolecules* **2013**, *46*, 4580; d) B. Sun, C. M. Jewell, N. J. Fredin, D. M. Lynn, *Langmuir* **2007**, *23*, 8452.
[18] a) J. Choi, M. F. Rubner, *Macromolecules* **2005**, *38*, 116; b) N. S. Zacharia, M. Modestino, P. T. Hammond, *Macromolecules* **2007**, *40*, 9523.
[19] H. Ochiai, Y. Anabuki, O. Kojima, K. Tominaga, I. Murakami, *J. Polym. Sci., Part B: Polym. Phys.* **1990**, *28*, 233.
[20] P. Bieker, M. Schönhoff, *Macromolecules* **2010**, *43*, 5052.
[21] P. Kujawa, P. Moraille, J. Sanchez, A. Badia, F. M. Winnik, *J. Am. Chem. Soc.* **2005**, *127*, 9224.
[22] J. J. Harris, P. M. DeRose, M. L. Bruening, *J. Am. Chem. Soc.* **1999**, *121*, 1978.